ISBN: 978-3-95450-249-3 ISSN: 2673-5350 doi: 10.18429/JACoW-IBIC2024-THP73

METHODOLOGY FOR IDENTIFYING THE CENTRE OF A SOLENOID MAGNET BASED ON THE BEAM DYNAMICS

Dong Hyuck Kim, Ji-Gwang Hwang*
Gangneung-Wonju National University, Gangneung, Republic of Korea

Abstract

The method of minimizing oscillation amplitude generated by varying the strength of a corrector magnet located upstream is commonly used for beam-based alignment of a single-pass machine. It minimises the amplitude of the centre of mass of the beams in beam diagnostics located downstream while the beam offset at the magnet is scanned by a corrector magnet upstream. The method is easily applied for a magnet capable of variable separation between horizontal and vertical planes such as a quadrupole magnet. However, in the case of a solenoid magnet, it is not suitable to apply the method since it has an azimuth magnetic component that produces mainly beam rotation. In this presentation, we propose an analytical method for identifying the centre of a solenoid magnet and present results validated by numerical simulations.

INTRODUCTION

In a practical situation, owing to the technical limits for the alignments and manufacturing imperfections, the centre of a magnet and the beam trajectory can not be aligned perfectly and the discrepancy originates a steering effect, additional focusing as well as nonlinear distribution. Therefore, during the machine operation, the offset is minimized using correctors installed in the beamline by adjusting the angle of the beam [1]. This procedure is so-called beam-based alignment (BBA). Particularly, in a linear machine, the BBA can be performed by minimizing the oscillation amplitude at a screen monitor downstream using a corrector upstream while the strength of the magnet is scanned [2]. It can be conducted based on the property of the separation of variables between two perpendicular axes in the motion of equations. However, the solenoid field, which is aligned with the beam axis introduces complexity in the beam dynamics, as the transverse motions in the x and y directions are coupled due to the solenoid field's nature. This coupling effect is the key difference from the uncoupled transverse dynamics observed in quadrupole magnets, where the x and y directions can be treated independently. This is not the case for solenoid magnets since they not only generate a strong x-y coupling but provide axisymmetric focusing properties due to the rotational symmetry of the magnetic field. The solenoids are widely used for low-energy electrons [3] and heavy ions because the focusing force is proportional to the beam radius and the structure can be easily enlarged to a large radius. In addition, providing the focus of both directions simultaneously is particularly advantageous in situations involving either the compact machine or low-energy injectors in which all elements are tightly installed in a narrow space. It was attempted to align the solenoid magnet with offline field measurement [4–6]. However, the offset between the magnet and the beam is inevitable during a machine operation driving the device. In this paper, we describe a theoretical approach to the alignment of the solenoid magnet. This presents a way to minimize the offset between the beam and the solenoid during the operation. This methodology has been proven by particle tracking simulations using the IMPACT-Z code [7].

* hwang@gwnu.ac.kr

A SOLENOID MAGNET

The understanding of the motion of charged particles in auxiliary fields, which is the core of accelerator physics, paves the way for controlling and manipulating particle beams precisely. Therefore, the basic equations for the solenoid magnet are revisited in the first part of this paper. With a hard-edge model, the solenoid field provokes a spiral motion, resulting in rotation in x-y space while propagating with a constant speed in the s-direction [8]. The magnetic field of the solenoid with steady currents can be derived by Ampère's law and can be expressed as follows

$$\oint \mathbf{B} \cdot d\mathbf{l} = \mu_0 I_{\text{enclosed}}, \tag{1}$$

where $I_{enclosed}$ represents the current enclosed by the amperian loop and μ_0 is the permeability of free space. In the case of an ideal solenoid, the magnetic field inside a solenoid is aligned along the axis of the solenoid, creating a uniform field within the central region. However, at the edges of the solenoid, the magnetic field begins to vary, forming what is known as the fringe field. Therefore, the magnetic field of the solenoid can be expressed as $\mathbf{B} = B_r(r,z)\hat{r} + B_z(r,z)\hat{z}$. This fringe field component B_r can have a significant impact on the motion of particles as they enter or exit the solenoid. In a solenoid, the magnetic field $\mathbf{B}$ can be represented by a vector potential $\mathbf{A}$ which can be calculated by

$$\oint \mathbf{A} \cdot d\mathbf{l} = \int \mathbf{B} \cdot d\mathbf{a}. \tag{2}$$

The vector potential of the solenoid is given by $\mathbf{A} = \frac{1}{2} r B_z \hat{\theta} = -\frac{B_z}{2} y\hat{x} + \frac{B_z}{2} x\hat{y}$. From the Maxwell Equation $\mathbf{B} = \nabla \times \mathbf{A}$, the radial magnetic field B_r which raises the focusing effect can be presented as

$$B_r = -\frac{\partial \mathbf{A}_\theta}{\partial z} = -\frac{1}{2} B_z' r, \tag{3}$$

In Eq. (3), there are two key points: (1) the radial magnetic field is proportional to the gradient of the axial magnetic field

ISBN: 978-3-95450-249-3 ISSN: 2673-5350 doi: 10.18429/JACoW-IBIC2024-THP73

B_z (2) the negative sign implies that B_r is directed inward as the axial magnetic field B_z decreases near the edge of the solenoid. To confirm the fringe field of the solenoid, the magnetic field of a solenoid with a length of 16 cm and a radius of 2.6 cm was computed using the Poisson Superfish code [9]. The result is shown in Fig. 1.

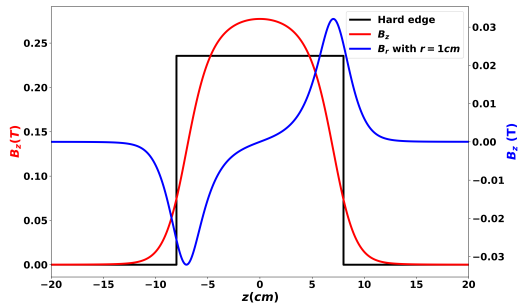

Figure 1: Schematic layout for identifying the centre of a solenoid magnet with a length of L. The beam arrives at the magnet with an offset of r and the screen monitor is distanced by l_d.

The equations of motion can be obtained by solving Hamilton's equations. Using this vector potential, the Hamiltonian **H** in $(x, p_x, y, p_y, z, \delta)$ coordinate for a relativistic charged particle with a mass of m and a charge of q moving in this magnetic field is given by [10–12]

$$H = \frac{\delta}{\beta_0} - \sqrt{F^2 - \sum_{i=x,y}\left(p_i - \frac{qA_i}{P_0}\right)^2 - \frac{1}{\beta_0^2\gamma_0^2}} - \frac{qA_z}{P_0}, \quad (4)$$

where $F = \left(\delta + \frac{1}{\beta_0} - \frac{q\phi}{cP_0}\right)$, $\delta = \frac{E}{cP_0} - \frac{1}{\beta_0}$, E is the total energy, P_0 is the total momentum, $\beta_0 = v/c$, γ is the Lorentz factor, ϕ represents the electrical potential, $\mathbf{p_x}$ and $\mathbf{p_y}$ denote the horizontal and vertical canonical momenta. The Hamiltonian includes both the kinetic energy of the particle and the interaction with the magnetic field via the vector potential. Using Hamilton's equations, the equations of motion for the particle in the solenoid ($\phi = 0$ and $A_z = 0$) can be derived as

$$\frac{\partial q}{\partial s} = \frac{\partial H}{\partial p_q}, \quad \frac{\partial p_q}{\partial s} = -\frac{\partial H}{\partial q}, \quad (5)$$

where the subscript q stands for x, y. Since the magnetic field in a solenoid is static, the equation of the motion can be solved for three regions at the entrance (field increases), body (constant), and exit (field decreases) of the magnet [13].

$$\mathbf{M_{exit}} = \begin{pmatrix} 1 & 0 & 0 & 0 \\ 0 & 1 & -kL & 0 \\ 0 & 0 & 1 & 0 \\ kL & 0 & 0 & 1 \end{pmatrix},$$

$$\mathbf{M_{entry}} = \begin{pmatrix} 1 & 0 & 0 & 0 \\ 0 & 1 & kL & 0 \\ 0 & 0 & 1 & 0 \\ -kL & 0 & 0 & 1 \end{pmatrix},$$

$$\mathbf{M_{body}} = \begin{pmatrix} 1 & \frac{\sin(kL)}{2k} & 0 & \frac{\sin^2(2kL)}{k} \\ 0 & \cos(2kL) & 0 & \sin(2kL) \\ 0 & \frac{\sin^2(kL)}{k} & 1 & \frac{\sin(2kL)}{2k} \\ 0 & -\sin(2kL) & 0 & \cos(2kL) \end{pmatrix},$$

with $k = B_z/(2B\rho)$, the magnetic rigidity of $B\rho$, and the effective length of the magnet L. The overall transfer matrix **M** is obtained by multiplying three distinct matrices $\mathbf{M} = \mathbf{M_{exit}} \cdot \mathbf{M_{body}} \cdot \mathbf{M_{entry}}$ [14];

$$\mathbf{M} = \begin{pmatrix} \cos^2\Phi & \frac{\sin 2\Phi}{2k} & \frac{\sin 2\Phi}{2} & \frac{\sin^2\Phi}{k} \\ -k\frac{\sin 2\Phi}{2} & \cos^2\Phi & -k\sin^2\Phi & \frac{\sin 2\Phi}{2} \\ -\frac{\sin 2\Phi}{2} & -\frac{\sin^2\Phi}{k} & \cos^2\Phi & \frac{\sin 2\Phi}{2k} \\ k\sin^2\Phi & -\frac{\sin 2\Phi}{2} & -k\frac{\sin 2\Phi}{2} & \cos^2\Phi \end{pmatrix}, \quad (6)$$

where $\Phi = kL$.

ANALYTICAL MODEL FOR IDENTIFYING THE CENTRE OF A SOLENOID

The basic layout for finding the magnetic field centre of a solenoid magnet consists of a screen monitor located downstream, as shown in Fig. 2. Then, with different beam offsets or angles, it is necessary to model the beam motion at the profile monitor while the strength of the magnet varies. With the centre of the incident beam of x_0 and y_0 as well

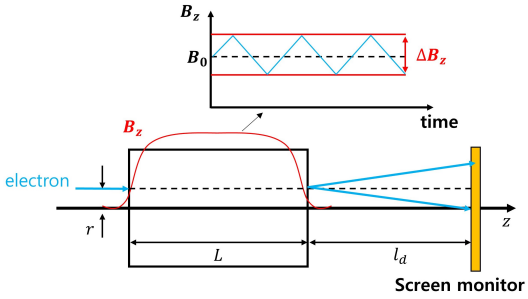

Figure 2: Schematic layout for identifying the centre of a solenoid magnet with a length of L. The beam arrives at the magnet with an offset of r and the screen monitor is distanced by l_d.

as without angles $x' = y' = 0$, the beam offset at the screen monitor can be derived from Eq. 6 for a solenoid strength of Φ and a travelling distance l_d from the solenoid to the screen monitor. The beam position x_s and x_s at the screen are given by

$$\begin{aligned} x_s &= \left(\cos^2\Phi - kl_d\sin\Phi\cos\Phi\right)x_0 \\ &\quad +(\sin\Phi\cos\Phi - kl_d\sin^2\Phi)y_0 \\ y_s &= \left(-\sin\Phi\cos\Phi + kl_d\sin^2\Phi\right)x_0 \\ &\quad +(\cos^2\Phi - kl_d\sin\Phi\cos\Phi)y_0. \end{aligned} \quad (7)$$

To demonstrate the equation, this result is compared with the macro-particle tracking simulation performed using the

ISBN: 978-3-95450-249-3 ISSN: 2673-5350 doi: 10.18429/JACoW-IBIC2024-THP73

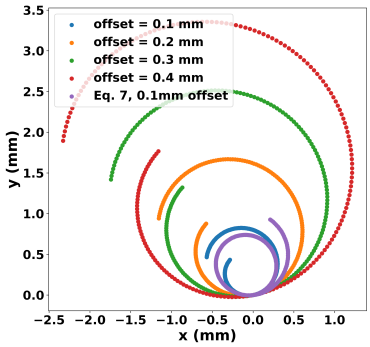

Figure 3: The motion of the beam centroid as a function of beam offset at the entrance of the solenoid. The solenoid has a strength of $B_z + \Delta B_z = 0.4 \pm 0.1$ T with a length of 0.25 m and a distance to the screen monitor of 0.25 m.

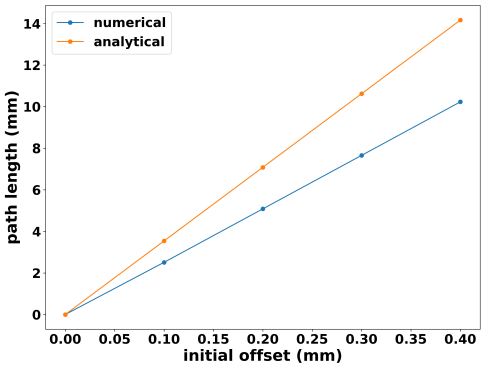

Figure 4: The path length of the circular motion at the screen monitor based on the analytical model in Eq. (8) and numerical simulations shown in Fig. 3.

IMPACT-Z code, which utilizes the nonlinear Lorentz integrator for the propagation of beams in magnetic elements.

As shown in Fig. 3, the centroid mainly moves around the circle in the real $(x-y)$ space. There is a slight difference between the formula and numerical simulations in terms of the radius changes since it involves the effect of the fringe field in the IMPACT-Z code. The solenoid in the Impact-Z code assumes that the fringe field region extended to twice the radius and, in addition, the magnetic field does not change linearly in this region, which increases the focusing strength. It also evidences that the radius of the circle at the screen monitor is proportional to the initial offset of the beam at the solenoid. In order to represent the radius change to a physical quantity, the path length at the screen monitor C is calculated by integrating the central travel path of the beam as a function of the strength. For a small strength variation Δk, i.e., $\Delta B_z << B_z$, it can be approximated as

$$\begin{aligned} C &= \int_{k_0}^{k_0+\Delta k} dk \sqrt{\left(\frac{\partial x_f}{\partial k}\right)^2 + \left(\frac{\partial y_f}{\partial k}\right)^2}, \\ &= r_0 \int_{k_0}^{k_0+\Delta k} dk L \sqrt{1 + k^2 l_d^2}, \\ &\approx r_0 \frac{L}{2 l_d} \ln\left(\frac{(k_0+\Delta k) l_d + \sqrt{1 + (k+\Delta k)^2 l_d^2}}{k_0 l_d + \sqrt{1 + k_0^2 l_d^2}}\right), \end{aligned} \quad (8)$$

where $r_0 = \sqrt{x_0^2 + y_0^2}$ denotes the initial offset. In Eq. (8), the path length is linearly proportional to the initial offset because the other terms are predefined in the beamline. In order to verify this fact, the path length for the circular motion is calculated based on the analytical model in Eq. (8) and numerical simulations shown in Fig. 3 and the numerical simulation, respectively, and the results are shown in Fig. 4. In both cases, the analytical model and the numerical simulation represent that the path length is linearly proportional to the initial beam offset. Therefore, the scanning of the path length with three offsets enables the identification of the beam offset close to the magnetic centre of the solenoid. This result also confirms that the slope of the numerical simulation with the IMPACT-Z code was slightly smaller than the analytical model. As shown in Fig. 3, the strong fringe field in the numerical simulation resulting in the great radius changes reduces the slope of the path length as a function of the initial offset.

CONCLUSIONS

The solenoid magnet, which is commonly used to focus the beam in low-energy injectors and heavy-ion machines, features the magnetic field component in the beam axis that triggers strong coupling between the x-y axes, making it difficult to apply the separation of variables in the beam-based alignment. In this study, we proposed the quantity of the path change of the central position at the screen monitor C in Eq. (8) that is only dependent on the initial offset while the strength of the solenoid is varying. It was also proved through theory and simulation that the path length increases monotonically on the initial offset. Therefore, measuring the C value at two or more corrector settings and extrapolating by a linear line will provide the strength for aligning the beam to the centre of the solenoid.

ACKNOWLEDGEMENT

This research was supported by the Basic Science Research Program through the National Research Foundation of Korea (NRF), funded by the Ministry of Education (RS-2023-00247042).

REFERENCES

[1] J.-G. Hwang *et al.*, "Analysis on effects of transverse electric field in an injector cavity of compact-ERL at KEK", *Nucl. Instrum. Methods Phys. Res., Sect. A*, vol. 753, pp. 97-104, Jul. 2014. doi:10.1016/j.nima.2014.03.045

[2] O. A. Tanaka, T. Miyajima, and T. Tanikawa, "Present status of the injector at the compact ERL at KEK", in *Proc. PAC'22*, Bangkok, Thailand, Jun. 2022, pp. 2296-2298. doi:10.18429/JACoW-IPAC2022-WEPOMS024

[3] J.-G. Hwang, E.-S. Kim, and T. Miyajima, "Effects of space charge in a compact superconducting energy recovery linac

ISBN: 978-3-95450-249-3 ISSN: 2673-5350 doi: 10.18429/JACoW-IBIC2024-THP73

with a low energy", *Nucl. Instrum. Methods Phys. Res., Sect. A*, vol. 684, pp. 18-26, Aug. 2012. doi:10.1016/j.nima.2012.03.042

[4] P. Arpaia, B. Celano, L. De Vito, A. Esposito, A. Parrella, and A. Vannozzi, "Measuring the magnetic axis alignment during solenoids working", *J. Manage. Sci. Rep.*, vol. 8, no. 1, Jul. 2018. doi:10.1038/s41598-018-29667-1

[5] P. Arpaia1, C. Petrone, S. Russenschuck, and L. Walckiers, "Vibrating-wire measurement method for centering and alignment of solenoids", in *Journal of Instrumentation*, vol. 8, no. 11, pp. P11006–P11006, Nov. 2013. doi:10.1088/1748-0221/8/11/p11006

[6] D. Arbelaez, J. W. Kwan, T. M. Lipton, A. Madur, and W. L. Waldron, "Magnetic Alignment of Pulsed Solenoids using the Pulsed Wire Method", in *Proc. PAC'11*, New York, NY, USA, Mar.-Apr. 2011, paper THOBS3, pp. 2087–2089. https://jacow.org/PAC2011/papers/THOBS3.pdf

[7] J. Qiang, R. D. Ryne, S. Habib, and V. Decyk, "An Object-Oriented Parallel Particle-In-Cell code for Beam Dynamics Simulation in Linear Accelerators", *J. Comput. Phys.*, vol. 163, no. 2, pp. 434-451, Sep. 2000. doi:10.1006/jcph.2000.6570

[8] S. M. Lund and Y. Hao, USPAS Accelerator Physics, Michigan State University, USA, 2021.

[9] M. T. Menzel and H. K. Stokes, *User's Guide for the POISSON/SUPERFISH Group of Codes*, Los Almos, NM, USA, Ja. 1987, LA-IR-87-115. https://uspas.fnal.gov/resources/Poisson_Superfish_Los_Alamos_Manual.pdf

[10] H. Wiedemann, "Beam Dynamics", in *Particle Accelerator Physics*. New York: Springer Berlin Heidelberg, 2007, pp. 49–59.

[11] S. Sheehy, "Particle Motion in EM Fields Lecture 1", presented at CERN Accelerator School, Budapest, Hungary, 2016, unpublished.

[12] Ph. Royer., "Solenoidal Optics", CERN, Geneva, Switzerland, Rep. PS/HP Note 99-12, Neutrino Factory Note 11, May 2000. https://cds.cern.ch/record/2849785/files/PS-HP-Note-99-12.pdf

[13] Sang-ho Kim and M. Doleans, "Principles of Superconducting Linear Accelerators,", in U.S. Particle Accelerator School, Duke University, Durham, NC, USA, 2013, unpublished.

[14] A.M. Lombardi, "Beam Lines,", presented at CERN Accelerator School, Zakopane, Poland, Oct. 2006, unpublished.